THE JOURNAL OF PHYSICAL CHEMISTRY C

Article

pubs.acs.org/JPCC

Electrical Double Layers near Charged Nanorods in Mixture Electrolytes

Zhou Yu, Haiyi Wu, and Rui Qiao*

Department of Mechanical Engineering, Virginia Tech, Blacksburg, Virginia 24061, United States

Supporting Information

ABSTRACT: The electrical double layers (EDLs) in the mixtures of room-temperature ionic liquids and water play an important role in many applications but have only begun to receive widespread attention recently. Here, we report the molecular dynamics simulations of EDLs near rigid polyanion nanorods immersed in electrolytes containing ionic liquids [C_2mim][TfO], water, and Na^+ ions. When the water content in bulk electrolyte is high, the EDLs near the rods are similar to those in aqueous electrolytes except that TfO^- ions accumulate notably near the cation layer adsorbed on the rods. When the water content in the bulk electrolyte becomes very low, even though water is greatly enriched in the interfacial region, the microenvironment in the region offers weak dielectric screening and the EDL exhibits features common to those in neat ionic liquids, e.g., charge overscreening. Na^+ ions are readily adsorbed on the sulfonate groups of the polyanion rod in the range of water contents explored here but can experience an energy barrier when moving from the bulk electrolyte to the rod surface if the water content is very low. Introducing Na^+ ions into the system displaces C_2mim^+ ions from the rod's surface. However, the number of displaced C_2mim^+ ions is far less than the Na^+ newly adsorbed on the rod, and thus, charge overscreening is enhanced. We highlight the important role of ion−ion correlations in determining the EDL characteristics and their response to the variation of mixture electrolytes' water/Na^+ ion contents revealed here and discuss their technical implications.

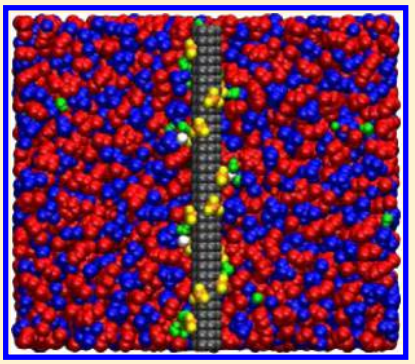

1. INTRODUCTION

An electrical double layer (EDL) is usually developed near a charged object in contact with electrolytes. Because of its important role in numerous applications such as micro-/nanofluidics and electrochemical energy storage, EDLs have been studied extensively.[1,2] Despite the diverse nature of electrolytes, all EDLs exhibit some common features; e.g., an EDL usually consists of a molecularly thin ion-free layer (called the Helmholtz layer or the Stern layer) and a diffuse layer spanning a few to thousands of nanometers. Nevertheless, previous research also established that the structure and macroscopic properties of EDLs depend strongly on the electrolyte's nature. There are four typical types of electrolytes: aqueous electrolytes, room-temperature ionic liquids (RTILs), high-temperature molten salts, and organic electrolytes. Aqueous electrolytes generally contain small inorganic ions (e.g., Na^+ and Cl^- ions) dissolved in water. Because of the high dielectric constant of water, the electrostatic interactions between ions are strongly screened, and ion−ion correlations are weak except when the surface charge density or the ion concentration is very high.[3−5] Consequently, the EDL structure can often be described satisfactorily by mean-field theories such as the Poisson−Boltzmann equation and its extensions.[6−8] RTILs usually feature bulky ions and contain no solvents. Because ions are in contact with each other, ion−ion correlations are especially strong in RTILs, and this leads to unique features for EDLs; e.g., counterions and co-ions form alternating layers near a charged surface, and surface charge is frequently overscreened.[1,9] While these features and the EDLs' macroscopic properties are difficult to describe using the classical EDL theories, they can be captured quite well by new theories that take into account the finite ion size and ion−ion correlations.[10−12] High-temperature molten salts also exhibit strong ion−ion correlation due to their solvent-free nature, and thus, EDLs in them resemble those in RTILs.[13] Organic electrolytes contain bulky ions dissolved in organic solvents, and they usually have low dielectric constants. Hence, the electrostatic interactions between ions are weakly screened, and ion−ion correlations are strong. Consequently, EDLs in organic electrolyte share some features with those in RTILs, e.g., charge overscreening.[14]

Most previous research focused on EDLs in the four types of neat electrolytes summarized above. However, there is a growing interest in studying EDLs in electrolyte mixtures. Many of these studies are motivated by the technical advantages offered by mixture electrolytes. For example, mixing ionic liquids and organic solvents can increase the mobility of ions and thus the power density of supercapacitors.[15−17] Some of these studies, however, are motivated by the practical issues inherent with neat electrolytes. For example, many RTILs are

Received: March 15, 2017
Revised: April 9, 2017
Published: April 12, 2017

ACS Publications © 2017 American Chemical Society

DOI: 10.1021/acs.jpcc.7b02466
J. Phys. Chem. C 2017, 121, 9454−9461

highly hygroscopic and thus inevitably contain some water, and clarifying the structure and properties of EDLs in such moist RTILs is important for the operation of supercapacitors based on RTILs. Molecular dynamics (MD) simulations showed that water molecules tend to accumulate within a subnanometer distance from electrified solid walls, although the structure of the EDL is not greatly affected by the adsorbed water molecules when the water concentration in bulk RTILs is low.[18,19] The adsorption of water molecules on the charged walls is determined by the gradient of electrical fields, the chemical nature of the ions near the wall, and the availability of space near the wall.[18] The influences of water on the interface between electrified RTIL and electrode have been investigated using in situ atomic force microscopy (AFM) and spectroscopy. The transition from a multilayered structure to a double-layer structure has been observed.[20]

In this work, we are interested in the EDLs near model polyelectrolytes immersed in mixture electrolytes consisting of RTILs, water, and small metal ions. Our interest is motivated by the recent synthesis of a new class of liquid crystalline ion gel in which rigid-rod polyanions are aligned in RTILs.[21] These gels exhibit an unusual combination of properties such as high ionic conductivity and strong mechanical cohesion, and they open up exciting new avenues for engineering ion conducting materials.[21] At present, such type of ion gel is fabricated through ion and water exchanged between a seed solution of aqueous polyelectrolyte solutions (e.g., 2,2′-disulfonyl-4,4′-benzidine terephthalamide, abbreviated as PBDT in literature; Na^+ ions were used as the counterion) and RTILs (e.g., 1-ethyl-3-methyl imidazolium trifluoromethane sulfonate, or [C_2mim][TfO]). Since the formation of these ion gels involves no chemical reactions, the EDLs surrounding the highly charged polyanions likely play a critical role in the gelation process, e.g., by regulating the interactions between the polyanions. Both the electrolyte and the polyanions in these ion gels exhibit a number of unique features that are not widely considered in previous studies of EDLs in mixture electrolytes. Specifically, most studies of EDLs in the RTIL mixture focused on situations in which where there is a small amount of water in RTILs and metal ions are rarely present. However, during the formation of the above ion gels, the electrolyte surrounding PBDT polyanions can contain more than 50% of water, and a large fraction of the polyanions' charge is balanced by the Na^+ ions. Furthermore, unlike the most widely studied situation in which solid surfaces are uniformly charged and homogeneous in chemical nature, polyanions feature discrete, hydrophilic sulfonate groups and neutral hydrophobic backbone. Because of these unique features, the structure and properties of the EDLs in the above ion gels are difficult extrapolate from prior studies of EDLs in mixture electrolytes, and many questions remain open. For example, how do water molecules, RTIL ions, and Na^+ ions distribute around the polyanion and how their distributions respond to the change in water and metal ion content in the bulk electrolyte? How are charges on the sulfonate groups of the polyanions screened and how do the bulky RTIL ions and the small Na^+ ions compete in screening the polyanions' charge?

Here, we seek to answer these questions by investigating the EDLs near isolated polyanion rods immersed in a mixture of RTILs, water, and Na^+ ions using MD simulations. The rest of the manuscript is organized as follows. The simulation system, molecular model, and methods are presented in section 2. Simulation results on the EDL structure are presented in section 3. Finally, conclusions are presented in section 4.

2. SIMULATION SYSTEM, MOLECULAR MODELS, AND METHODS

Figure 1 shows a schematic of the MD system, which consists of a single PBDT rod fixed in the center of a simulation box and

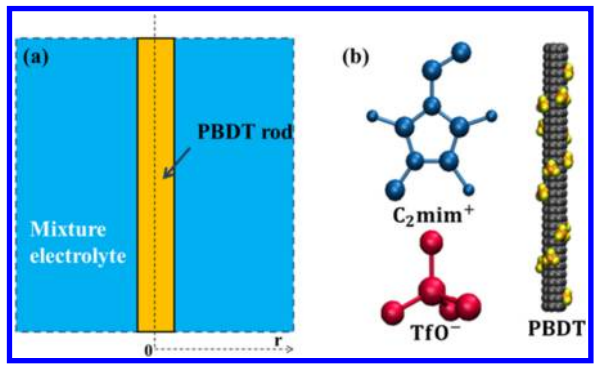

Figure 1. Schematics of the simulation system (a) and the molecular structure of the C_2mim$^+$, TfO$^-$ ion, and the semicoarse grained PBDT rod (b). (b) Orange (yellow) balls denote the sulfur (oxygen) atoms of the sulfonate groups of the PBDT rod.

the accompanying electrolytes. The electrolyte was a mixture of RTILs [C_2mim][TfO], water, and Na^+ ions (in some cases, Na^+ ions were not added; see Table 1). The simulation box was

Table 1. Setup of the MD Systems Studied in This Work

system	C_2mim$^+$ no.	TfO$^-$ no.	water no.	Na^+ no.	Na^+/SO_3^- ratio	$x_{w,\infty}$ [a]
1	1326	1316	96	8	0.5	0.02
2	1297	1287	381	8	0.5	0.11
3	1241	1231	939	8	0.5	0.24
4	1152	1142	1841	8	0.5	0.42
5	984	974	3536	8	0.5	0.62
6	554	544	7927	8	0.5	0.87
7	1157	1137	1841	0	0.0	0.42
8	1147	1147	1841	16	1.0	0.42

[a] $x_{w,\infty}$ is the mole fraction of water in region 3.5−4.0 nm from the rod axis where the electrolyte is bulklike.

6.72 nm in the z-direction (i.e., along the PBDT rod's axis). The simulation box was 8.00 nm in both x- and y- directions, which is large enough to obtain a bulklike behavior at the position away from the PBDT rod. Hereinafter, the mole fraction of water in the region 3.5−4.0 nm from the rod axis will be referred to as the mole fraction of water in bulk mixture electrolyte, $x_{w,\infty}$. In as-fabricated ion gels, the average spacing between neighboring PBDT rods can range from a few nanometers to tens of nanometers depending on the fabrication conditions,[21] and hence, EDLs around different PBDT rods may or may not interact with each other. Here, we focus on the situation where the EDLs around individual rods are independent of each other, and the insight gained in the present system will form the basis of future studies.

The number of C_2mim$^+$, TfO$^-$, and Na^+ ions and water molecules inside the system were chosen to meet two criteria simultaneously. First, the system is electrically neutral. Second, at positions outside of the EDL, we achieve different water mole fraction of the mixture electrolyte ($x_{w,\infty}$) while ensuring

DOI: 10.1021/acs.jpcc.7b02466
J. Phys. Chem. C 2017, 121, 9454−9461

that the density of the mixture electrolyte is equal to bulk mixture electrolyte with the same water mole fraction (see Figure S1 and Table S1 for the density of mixture electrolyte as a function of water mole fraction). Table 1 summarizes the setup of the MD systems studied in this work.

The PBDT polyanions were described using a semicoarse grained model. Prior experiments indicated that PBDTs self-assemble into rigid rods with helical structures.[21,22] Here, we model the self-assembled PBDT rods as rigid rods decorated with explicitly resolved sulfonate groups (see Figure 1b). Briefly, each PBDT rod consists of four 1.68 nm long repeating units. Each repeating unit is made of nine layers of carbon atoms arranged into a regular heptagon, and four sulfonate groups are anchored on the carbon atoms in different layers. Further details about the PBDT model can be found in our prior work.[23] Overall, the backbone of the PBDT rod has a radius of ~0.2 nm and a linear charge density of −2.38 e/nm. The simple model adopted here captures PBDT rods' key geometrical and chemical features, e.g., their semirigid structure, the hydrophobic nature of their backbone, and the discrete distribution of sulfonate groups along their contour length. The force fields for the C_2mim^+ and TfO^- ions were taken from ref 24, which were developed within the framework of the AMBER/OPLS force fields. As demonstrated in our prior studies, the simple PBDT model and the RTIL force fields adopted here allow reasonable prediction of the dynamics of ions in PBDT-based ion gels.[23] Water was modeled using the SPC model, and the Na^+ ions were modeled using the OPLS-AA force field.[25,26] We note that prior studies showed that using the OPLS-AA force fields for Na^+ ion and the SPC water model together can reproduce key properties of Na^+ ion hydration in water.[26] Furthermore, separate simulation of bulk mixture of water and $[C_2mim][TfO]$ indicated that these fluids are miscible as observed experimentally.

Simulations were performed using the Gromacs code[27] with a 2 fs time step. All simulations were executed in the NVT ensemble. To ensure effective sampling of the phase space, simulations were performed at an elevated temperature of 353.15 K, which is common in simulation of RTILs. The temperature of the system was maintained at the target temperature using the velocity rescaling thermostat.[28] The nonelectrostatic interactions were computed by direct summation with a cutoff length of 1.2 nm. The electrostatic interactions were computed using the Particle Mesh Ewald (PME) method. The real space cutoff and FFT spacing were 1.2 and 0.12 nm, respectively. All bonded interactions were computed except that the length of the C−H bonds were constrained using the LINCS algorithm.[29]

For systems with high water mole fraction (systems 3−8 in Table 1), water molecules, Na^+ ions, and RTIL ions were first randomly packed inside the system. Starting from such initial configurations, each system was equilibrated for 20 ns, during which many exchanges between Na^+ ions adsorbed on the PBDT rod and residing in the bulk electrolyte were observed. The equilibration run was then followed by a 100 ns production run. For systems with low water mass fraction (systems 1 and 2 in Table 1), we found that the above process is not sufficient to lead to effective sampling of the Na^+ ions distribution near the PBDT rods because they must overcome a large energy barrier to become adsorbed on the PBDT rods. Therefore, for these systems, Na^+ ions were first packed near the PBDT rods and systems were run for 5 ns. Next, RTILs and water molecules were introduced into the system and the system was equilibrated for 40 ns. This was then followed by a production run of 100 ns.

3. RESULTS AND DISCUSSION

3.1. Evolution of EDL with the Water Content of Mixture Electrolytes. We first examine the EDL structure in systems 1−6 in Table 1 in which the mole fraction of water in the bulk mixture electrolyte, $x_{w,\infty}$, is varied from 0.02 to 0.87. In these systems, 50% of the negative charge on the PBDT rod is balanced by C_2mim^+ and TfO^- ions and the rest is balanced by the Na^+ ions. Figure 2a shows that, at $x_{w,\infty}$ = 0.87, water

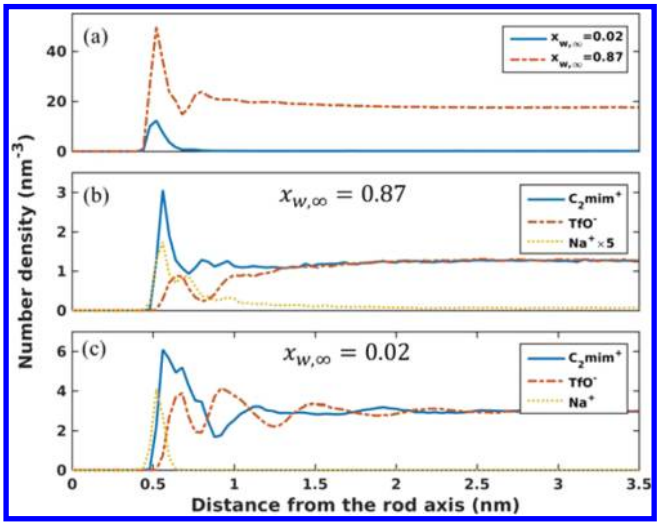

Figure 2. (a) Density distribution of water molecules around the PBDT rod for $x_{w,\infty}$ = 0.02 and 0.87. (b, c) Density distribution of the C_2mim^+, TfO^-, and Na^+ ions as a function of their radial distance from the PBDT rod axis when mole fraction of water molecules in the bulk mixture electrolyte is $x_{w,\infty}$ = 0.87 (panel b) and $x_{w,\infty}$ = 0.02 (panel c). In panels, the position of any molecule is based on its center-of-mass. The density of Na^+ ions is multiplied by a factor of 5 for clarity in (b). Similar results for other values of $x_{w,\infty}$ are shown in Figure S2.

molecules exhibit clear layering near the rod as commonly observed for liquids in contact with solid objects. The water density becomes relatively uniform at position ~1.5−2 nm from the rod. Given the high density of the water molecules throughout the system, the C_2mim^+ and TfO^- ions are essentially bulky organic ions dissolved in water. Figure 2b shows that the C_2mim^+ ion density exhibits a distinct peak at r = 0.56 nm, but it becomes nearly uniform at positions ~1.5 nm away from the rod. As expected, near the negatively charged rod, the TfO^- ion density is lower than its bulk value. However, a significant accumulation of TfO^- ions near the rod, evident from the peak located at r = 0.68 nm, is observed. This accumulation originates from the electrostatic attraction by the C_2mim^+ ions adsorbed on the rod. In this system, the electrostatic interactions between these ions are screened rather strongly by the water molecules. Nevertheless, because these bulky ions interact much more weakly with their hydration water molecules compared to small inorganic ions such as Na^+ and Cl^-, they can form contact ion pairs by shedding part of their hydration shell. Consequently, the correlations between the C_2mim^+ and TfO^- ions are still strong enough to induce the notable peak of the TfO^- ion at r = 0.68 nm. Figure 2b also shows that Na^+ ion density shows a peak at r = 0.56 nm but it does not decrease monotonically as we move

DOI: 10.1021/acs.jpcc.7b02466
J. Phys. Chem. C 2017, 121, 9454−9461

away from the rod. Instead, weak plateaus at r = 0.72 and 0.96 nm are observed. These plateaus are likely caused by the electrostatic attractions by the TfO^- ions located in the peak at r = 0.68 nm and in the weak plateau at $r \approx 1.00$ nm.

As water is removed from the mixture electrolyte, the electrolyte transitions gradually from RTILs dissolved in water to water dissolved in RTILs, and the structure of the EDL changes as a result (see Figure S2). Here, we examine the EDL structure at $x_{w,\infty}$ = 0.02 in detail, when the electrolyte is best considered as moist RTILs. Figure 2a shows that water molecules are greatly enriched within a radius of ~0.7 nm from the rod axis. This enrichment is caused mainly by the strong hydrophilicity of the sulfonate groups on the PBDT rod. Comparison of the ion distribution in Figure 2b,c shows that when the water content of the electrolyte is greatly reduced the C_2mim^+ ion density peak grows both wider and higher. This is because, at low water mole fraction, C_2mim^+ ions appear near the rod surface not only because of the electrostatic attraction by the rod's negative charge but also because, as a liquid, the RTILs tend to form well-defined layers near solid surfaces. Figure 2c shows that TfO^- ions form alternating layers with the C_2mim^+ ions near the rod, thus exhibiting one of the universal features of the EDLs in RTILs.[1] Interestingly, we observe that nearly all Na^+ ions become contact adsorbed on the PBDT rod (see also Figure 4b). The strong preference of the Na^+ ions to the PBDT rod over bulk RTILs is a result of the interplay between its hydration by water molecules and electrostatic attractions by the sulfonate groups on the PBDT rod.

In addition to ion distributions, we also investigated the EDLs near the rod by computing how the charge on the rod is screened by the RTIL and Na^+ ions. Specifically, we computed the charge screening factor β as a function of radial distance r from the rod axis

$$\beta(r) = -\frac{1}{q_L}\int_0^r 2\pi r \rho_e(s)\, ds \qquad (1)$$

where $\rho_e(s)$ is space charge density due to ions at a radial distance s and q_L is the charge on the PBDT rod per unit length (−2.38 e/nm). At positions with $\beta > 1.0$, the surface charge on the rod is overscreened. Charge overscreening is a universal feature of the EDLs in RTILs and many organic electrolytes.[1,10] Figure 3 shows that, at $x_{w,\infty}$ = 0.87, the rod's charge is fully screened at a distance of ~2.0 nm from the rod's axis (thus the EDL is ~2.0 nm thick) and overscreening does not occur. As $x_{w,\infty}$ decreases, the EDL is compressed, and overscreening becomes obvious for $x_{w,\infty} \leq 0.42$. Overall, this is consistent with the fact that, as $x_{w,\infty}$ decreases, the electrolyte becomes more concentrated and behaves more like a RTIL, in which overscreening is usually observed.

We have so far focused on the average distribution of ions in the radial direction of the rod. This allows us to focus on the EDL's long-range structure, but its neglects the variation of ion densities in the circumferential and rod axis directions. However, since the charge of a PBDT rod is distributed discretely on its sulfonate groups, it is instructive to study how ions and water molecules distribute near individual sulfonate groups to gain insight into the EDL structure at short range. To this end, we computed the radial density distributions of C_2mim^+, TfO^-, Na^+ ions, and water molecules around PBDT's sulfonate groups (see Figure 4 and Figure S3). Figure 4a shows that, at $x_{w,\infty}$ = 0.87, the sulfonate groups are well hydrated by water molecules. The distribution of C_2mim^+ and TfO^- ions

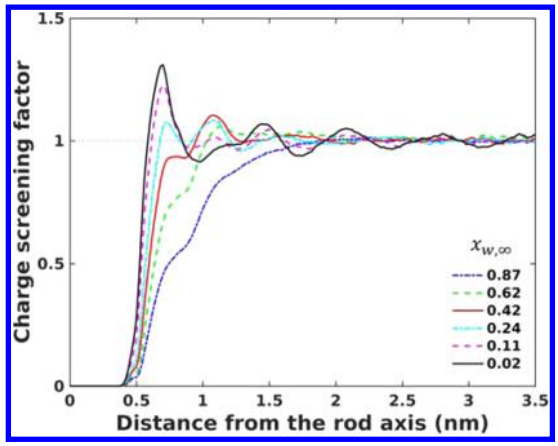

Figure 3. Variation of the charge screening factor as a function of the radial distance from the PBDT rod axis for different water mole fractions in the bulk mixture electrolyte. The ratio of the number of Na^+ ions in the electrolyte and the number of sulfonate group on the PBDT rod is 0.5.

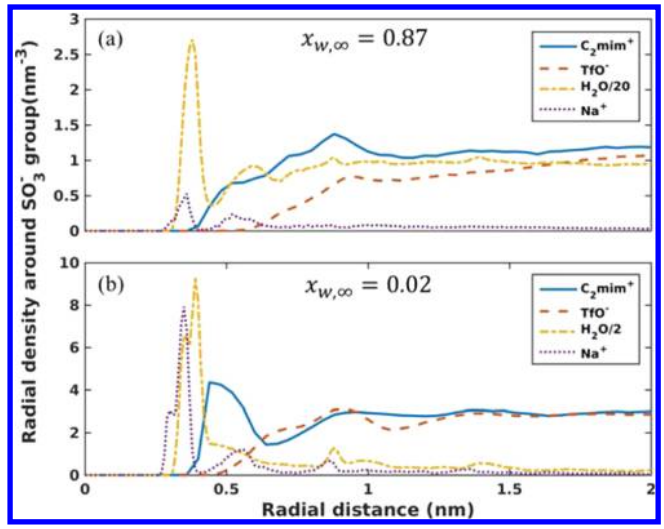

Figure 4. Radial density profiles of the C_2mim^+, TfO^-, and Na^+ ions and water molecules as a function of the their distance to the sulfonate groups on the PBDT rods when the mole fraction of water in the bulk mixture electrolyte is $x_{w,\infty}$ = 0.87 (panel a) and $x_{w,\infty}$ = 0.02 (panel b). The sulfur atom of the sulfonate group is taken as the origin. In (a) and (b), the density of water molecules is divided by a factor of 20 and 2, respectively. Similar results for other values of $x_{w,\infty}$ are shown in Figure S3.

are rather diffusive around the sulfonate group, with few C_2mim^+ ions contact adsorbed on the sulfonate group. However, as indicated by density peak at a radial distance of 0.38 nm, many Na^+ ions are contact adsorbed on the sulfonate group. Hence, Na^+ ions are more competitive than the C_2mim^+ ions in screening the sulfonate groups' charge. Figure 4b shows that, at $x_{w,\infty}$ = 0.02, each sulfonate group is hydrated roughly by one shell of water molecule around them. Figure 4b and visualization of the trajectory indicate that this single shell of water molecules does not seal the sulfonate group from the ions. Instead, it is penetrated by both Na^+ ions and C_2mim^+ ions contact adsorbed on the sulfonate group. The much stronger adsorption of Na^+ and C_2mim^+ ions on the sulfonate groups as $x_{w,\infty}$ decreases from 0.87 to 0.02 is consistent with the transition of the microenvironment near the sulfonate groups from water-rich to RTIL-rich.

DOI: 10.1021/acs.jpcc.7b02466
J. Phys. Chem. C 2017, 121, 9454−9461

For applications such as preparation of ion gels through ion exchange, it is important to know the exchange between Na^+ ions adsorbed on the PBDT rods and in bulk electrolytes.[21] Therefore, we study the thermodynamics of such exchange and how it depends on the water content of the mixture electrolyte. Specifically, we computed the potential of mean force (PMF) of Na^+ ions as a function of its distance to the rod axis. In electrolytes with high water content ($x_{w,\infty} \geq 0.24$), the exchange between adsorbed and free Na^+ ions can be sampled effectively in our simulations, and thus the Na^+ density away from the rod can be computed very accurately. Therefore, the PMF was computed from the radial ion distribution profile using $PMF(r) = -k_BTIn(\rho_n(r)/\rho_{n,\infty})$, where k_B is Boltzmann's constant and T is the absolute temperature. $\rho_n(r)$ is the Na^+ ion number density at a radial distance of r from the rod axis (see Figure 2). $\rho_{n,\infty}$ is the density of Na^+ ions outside of the EDL, where the PMF is taken as zero. In electrolytes with low water content, the above method cannot compute the PMF reliably because Na^+ ions are adsorbed on the PBDT rods most of the time, and thus, it is difficult to accurately determine $\rho_n(r)$ at large r. To resolve this difficulty, we computed the PMF using the umbrella sampling method.[30,31] We first generated a series of configurations each with a different radial Na^+−rod separations. Next, a harmonic potential (force constant: 1000 kJ/(mol·nm^2)) was applied to the Na^+ ion to constrain its radial distance from the PBDT rod's axis. A 20 ns long equilibrium simulation was performed under this constraint for each configuration, and the position of the Na^+ ion was recorded. Finally, the PMF of the Na^+ ion was extracted from the histograms of its position in the different runs using the Weighted Histogram Analysis Method implemented in the Gromacs code.[31,32]

Figure 5 shows Na^+ ion's PMF profiles in three representative mixture electrolytes (data for other electrolytes

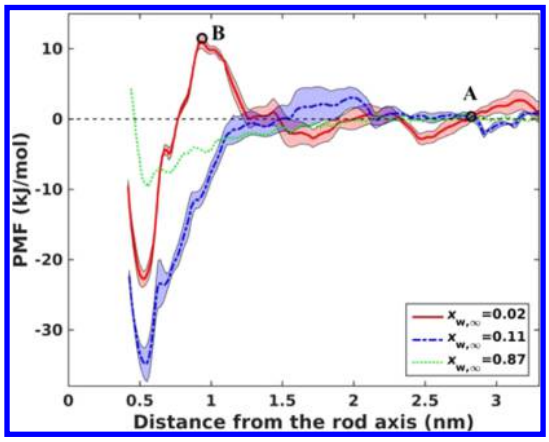

Figure 5. Potential of mean force (PMF) of Na^+ ions as a function of their distance from the PBDT rod axis when the bulk mixture electrolytes have different water contents. In each case, the PMF of Na^+ ions located at a position far away from the rod is taken as zero. The shaded regions around the PMF curves denote the uncertainties in the PMF.

are shown in Figure S4). In all cases, a PMF valley is observed for Na^+ ions near the rod. The depth of this valley increases as $x_{w,\infty}$ decreases from 0.87 to 0.11 but then decreases as $x_{w,\infty}$ decreases from 0.11 to 0.02. Interestingly, while the PMF usually decreases monotonically as the Na^+ ion moves toward the rod axis, in the electrolyte with the lowest water content ($x_{w,\infty}$ = 0.02), an energy barrier is observed at a radial distance of ∼0.95 nm from the rod axis.

The existence of a PMF valley near the PBDT rod is consistent with the strong adsorption of Na^+ ions on the PBDT rods. As $x_{w,\infty}$ decreases, the liquid medium surrounding the rod transitions from an aqueous electrolyte to a moist RTIL and its dielectric screening ability reduces. Therefore, the Na^+ counterions are attracted electrostatically toward the rod more strongly, leading to a deeper PMF valley. As $x_{w,\infty}$ reaches very low value (e.g., 0.02), water molecules are greatly enriched at the rod-electrolyte interfaces compared to bulk electrolytes (see Figure 2a). As such, the Na^+ ions near the rod reside in a microenvironment in which its electrostatic interactions with other ions are screened more strongly than in bulk electrolytes. Such an effect tends to reduce the depth of the PMF valley. Because the enrichment of water molecules at the rod-electrolyte interface is more significant in electrolyte containing little water, this effect is more prominent as $x_{w,\infty}$ reaches a very small value, and it likely contributes to the reduction of the PMF valley observed as $x_{w,\infty}$ decreases from 0.11 to 0.02.

At the lowest $x_{w,\infty}$ studied here, the Na^+ ions' PMF oscillates as we move from bulk electrolytes toward the rod, and an energy barrier appears in the region 0.75 nm < r < 1.25 nm. Since previous work on the EDLs in neat RTILs showed that the short-range correlations between ions are more important in leading to oscillatory PMF,[10,33] we analyzed the distribution of molecules around Na^+ ions located in the bulk electrolyte and at the peak of the energy barrier, and the results are shown in Figure 6. Comparison of the distributions of ions and water

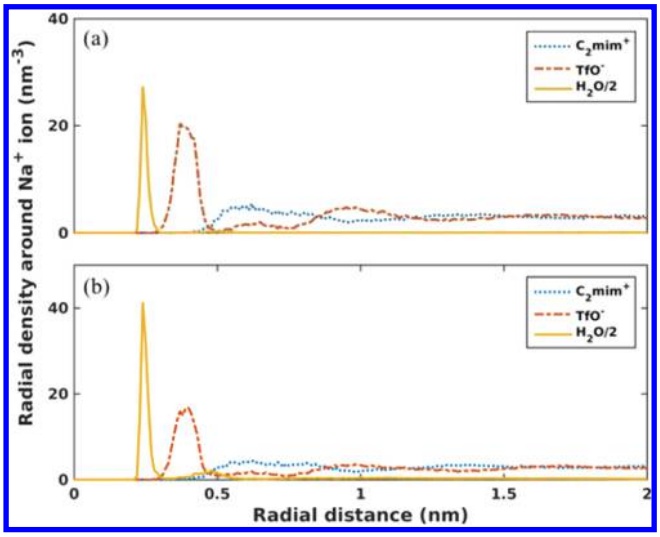

Figure 6. Radial density distribution of C_2mim^+, TfO^- ions, and water molecules around Na^+ ions located at radial distances of 2.8 nm (panel a, corresponding to point A in Figure 5) and 0.95 nm (panel b, corresponding to point B in Figure 5) from the PBDT rod's axis. The mole fraction of water in the bulk mixture electrolyte is 0.02.

molecules around Na^+ ions shown in Figure 6a,b shows that, as a Na^+ ion moves from the bulk electrolyte (point A in Figure 5) toward the PMF peak (point B in Figure 5), more water molecules (less TfO^- ions) appear near it. Calculation of the Na^+ ion's coordination number (i.e., the number of water molecules or ions within the first peak of the radial distribution function) shows that the number of coordination water molecules increases from 1.15 to 1.83, while that of the coordination TfO^- ions reduces from 3.57 to 3.04. While the

DOI: 10.1021/acs.jpcc.7b02466
J. Phys. Chem. C 2017, 121, 9454−9461

decrease of Na^+ ion's coordination by TfO^- ions is comparable to the increase of the coordination by water molecules, the loss of energy due to less Na^+-TfO^- interactions should be more significant than the gain of energy due to more Na^+–water interactions because charge–charge interactions are usually stronger than charge–dipole interactions. Hence, it is reasonable to attribute the appearance of the energy barrier in 0.75 nm < r < 1.25 nm to the reduced coordination of Na^+ ions by the TfO^- ions.

3.2. Evolution of EDL with Counterion Composition of Mixture Electrolytes. Above, we focused on EDLs in which the Na^+ ions in the mixture electrolytes balance 50% of the PBDT rod's charge. In practice, the amount of Na^+ ions in the mixture electrolytes can often be controlled; e.g., in the fabrication of ion gels, the amount of residual Na^+ ions in the ion gel can be tuned by varying the volume of the RTIL solution used to exchange Na^+ ions from the seed solution containing PBDT. Here, we examine how the Na^+ ion content of the mixture electrolyte affects the EDL structure around the PBDT rods. This was achieved by replacing the C_2mim^+ ions in a Na^+-free mixture electrolytes by Na^+ ions or, in another words, by varying the ratio between the number of Na^+ ions in the electrolyte and the number of sulfonate groups on the PBDT rod (Na^+/SO_3^-). Since the water content of as-fabricated gel is usually not very low, we fixed the mole fraction of water in bulk mixture electrolyte to be 0.42.

Figure 7 shows the distribution of water molecules, C_2mim^+, TfO^-, and Na^+ ions at Na^+/SO_3^- ratio of 0, 0.5, and 1.0. We

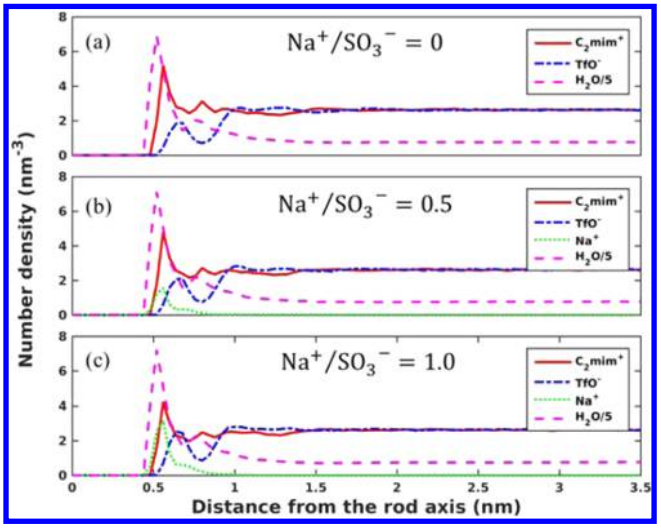

Figure 7. Comparison of the density distribution of ions and water molecules around the PBDT rod when the ratio of the number of Na^+ ions in the electrolyte and the number of the sulfonate group on the PBDT is 0, 0.5, and 1. The mole fraction of water in the bulk mixture electrolyte is fixed at $x_{w,\infty}$ = 0.42. The density of water molecules is divided by a factor of 5 for clarity.

observe that for a Na^+/SO_3^- ratio of 0.5:1.0 the Na^+ density in bulk electrolytes (i.e., large radial distance from the rod) is much lower than that in the interfacial zone near the rod. However, the *absolute* Na^+ density (~18 mM in Figure 7c) in the bulk electrolyte is far from zero. Since the volume of the interfacial zone is much smaller than that of bulk electrolytes, the fraction of Na^+ ions in the interfacial zone (e.g., within 1.0 nm from the rod axis) is much lower than 100% (~66% in the system corresponding to Figure 7c). Therefore, the Na^+ ion density profiles in Figure 7 are consistent with the experimental observation that Na^+ ions can be exchanged out of the seed solution when making ion gels using the method developed in ref 21.

Figure 7 shows that introducing Na^+ ions into the electrolyte causes little change in the water distribution near the rod. Many of the introduced Na^+ ions become adsorbed on the PBDT rods. Meanwhile, the density of C_2mim^+ ions near the rod decreases. This is consistent with the idea that Na^+ ions are more competitive than C_2mim^+ ions in adsorbing onto the sulfonate groups of the PBDT rod, as already inferred from Figure 4a. However, the decrease of the C_2mim^+ ion density, especially the first C_2mim^+ peak, is much smaller than the increase of Na^+ ion density near the rod, and the density of TfO^- ions near the rod also increases moderately. These observations can be understood as follows. Due to the weak dielectric screening by the mixture electrolyte, there exists strong short-range correlation between cations and anions due to their electrostatic attraction. Because Na^+ ions are smaller than the C_2mim^+ ions, the Na^+-TfO^- correlations are stronger than the $C_2mim^+-TFO^-$ correlations. When N number of C_2mim^+ ions adsorbed on the PBDT rods are replaced by N number of Na^+ ions, these Na^+ ions bring additional TfO^- ions toward the PBDT rods, which in turn helps bring some C_2mim^+ ions toward the PBDT rod due to short-range correlations between TfO^- and C_2mim^+ ions. Therefore, the increase of Na^+ ion density near the rod is larger than the decrease of C_2mim^+ ion density in the same region.

A key consequence of the above observations is that charge overscreening is enhanced as Na^+ ions replace C_2mim^+ ions (or equivalently, as Na^+/SO_3^- increases). This is evident in Figure 8. Since charge overscreening can greatly affect the effective

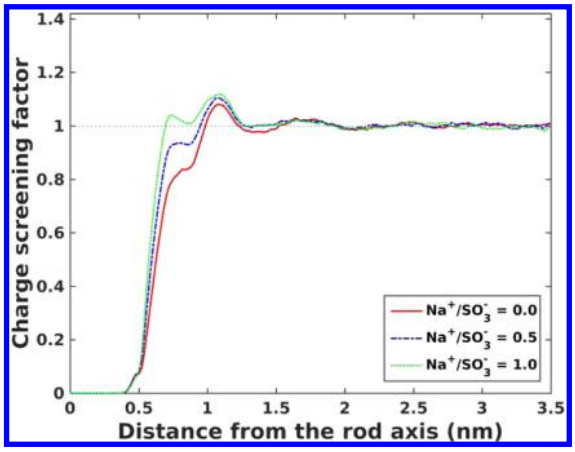

Figure 8. Comparison of the charge screening factor when the ratio of the number of Na^+ ions in the electrolyte and the number of sulfonate group on the PBDT rod is 0, 0.5, and 1. The mole fraction of water in the bulk mixture electrolyte is fixed at 0.42.

interactions between charged objects immersed in electrolytes (e.g., sometimes leading to attraction between like-charged objects[34]), the present results suggest that a small amount of Na^+ ions can potentially change the stability of polyanion rods in mixture electrolytes. Exploring such effects is important for understanding the thermodynamics and kinetics of ion gel formation and will be pursued in future studies.

DOI: 10.1021/acs.jpcc.7b02466
J. Phys. Chem. C 2017, 121, 9454–9461

4. CONCLUSIONS

In summary, we studied the EDLs near charged PBDT polyanion rods immersed in mixture electrolytes featuring $[C_2mim][TfO]$, water, and Na^+ ions using molecular dynamics simulations. At large water mole fractions, the electrolyte behaves like an aqueous solution of bulk organic ions. The EDL shares similarity with that in typical aqueous electrolytes, and charge overscreening does not occur. Nevertheless, the correlations between C_2mim^+ and TfO^- are still strong enough to induce notable accumulation of TfO^- ions near the C_2mim^+ ions contact adsorbed on the charged rod. At very low water mole fraction, the bulk electrolyte behaves like moisturized RTILs. However, water is enriched near the rod surface. Even in the driest electrolyte considered here ($x_{w,\infty}$ = 0.02), each sulfonate group on the PBDT rod is hydrated by one shell of water molecules. Nevertheless, because the dielectric screening of interfacial water is much weaker than in water-rich electrolytes, the C_2mim^+ peak near the rod becomes both wider and higher as water is removed from the electrolyte, and the EDL exhibits features common to EDLs in RTILs, e.g., alternative layering of C_2mim^+ and TfO^- ions and charge overscreening. We also found that, regardless of the water content of the electrolyte, Na^+ ions strongly favors the interfacial region and are always more competitive than the C_2mim^+ ions in adsorbing on the PBDT' sulfonate groups. For electrolytes with moderate water contents, some C_2mim^+ ions are displaced from the rod's surface as Na^+ ions are introduced into the system. However, the amount of displaced C_2mim^+ ions is far smaller than that amount of introduced Na^+ ions because of the strong Na^+-TfO^- and $C_2mim^+-TFO^-$ correlations. Despite that Na^+ ions always favors the rod's surface, in electrolytes with very low water content (e.g., $x_{w,\infty}$ = 0.02), Na^+ ions must overcome an energy barrier when moving from bulk electrolyte to adsorb on the PBDT rod. This is because, compared to the Na^+ ions in the bulk electrolyte, while Na^+ ions near the rod are better hydrated by more water molecules, they are surrounded by less TfO^- ions.

Overall, our simulations showed that, in RTIL–water mixture electrolytes, the structure of EDL is affected by the correlations between C_2mim^+ and TfO^- ions. Such an effect weakens as the water content increases but it cannot be neglected even when the water mole fraction in bulk electrolyte reaches 0.87. The correlations between the Na^+ ions and the TfO^- ions, along with those between the C_2mim^+ and TfO^- ions, leads to the enhanced charge overscreening when a small amount of Na^+ ions are introduced into the electrolyte. This suggests that manipulating of the Na^+ content in mixture electrolytes can be a potent strategy for tuning the charge overscreening of polyanion rods and potentially the interactions between polyanion rods.

■ ASSOCIATED CONTENT

Supporting Information

The Supporting Information is available free of charge on the ACS Publications website at DOI: 10.1021/acs.jpcc.7b02466.

Density of RTIL and water mixture, the Lennard-Jones parameters and atom charge for PBDT atoms, the (radial) distribution of C_2mim^+, TfO^-, Na^+ ions, and water molecules around the rod axis (around the sulfonate groups) with different water contents in the mixture electrolyte, and PMF profiles of Na^+ ions (PDF)

■ AUTHOR INFORMATION

Corresponding Author

*E-mail: ruiqiao@vt.edu.

ORCID

Rui Qiao: 0000-0001-5219-5530

Notes

The authors declare no competing financial interest.

■ ACKNOWLEDGMENTS

This work was partially supported by the US National Science Foundation under Award No. CBET 1264578. We thank the ARC at Virginia Tech for generous allocations of computer time on the BlueRidge and NewRiver cluster.

■ REFERENCES

(1) Fedorov, M. V.; Kornyshev, A. A. Ionic liquids at electrified interfaces. *Chem. Rev.* **2014**, *114*, 2978–3036.

(2) Israelachvili, J. N. *Intermolecular and surface forces*; Academic Press, 2011.

(3) Grønbech-Jensen, N.; Mashl, R. J.; Bruinsma, R. F.; Gelbart, W. M. Counterion-induced attraction between rigid polyelectrolytes. *Phys. Rev. Lett.* **1997**, *78*, 2477.

(4) Moreira, A. G.; Netz, R. R. Strong-coupling theory for counter-ion distributions. *Europhys. Lett.* **2000**, *52*, 705.

(5) Xu, D.; Li, D.; Leng, Y.; Chen, Y. Molecular dynamics simulations of ion distribution in nanochannels. *Mol. Simul.* **2007**, *33*, 959–963.

(6) Bazant, M. Z.; Thornton, K.; Ajdari, A. Diffuse-charge dynamics in electrochemical systems. *Phys. Rev. E* **2004**, *70*, 021506.

(7) Kilic, M. S.; Bazant, M. Z.; Ajdari, A. Steric effects in the dynamics of electrolytes at large applied voltages. II. Modified Poisson-Nernst-Planck equations. *Phys. Rev. E* **2007**, *75*, 021503.

(8) Bazant, M. Z.; Kilic, M. S.; Storey, B. D.; Ajdari, A. Towards an understanding of induced-charge electrokinetics at large applied voltages in concentrated solutions. *Adv. Colloid Interface Sci.* **2009**, *152*, 48–88.

(9) Kornyshev, A. A. Double-layer in ionic liquids: paradigm change? *J. Phys. Chem. B* **2007**, *111*, 5545–5557.

(10) Bazant, M. Z.; Storey, B. D.; Kornyshev, A. A. Double layer in ionic liquids: Overscreening versus crowding. *Phys. Rev. Lett.* **2011**, *106*, 046102.

(11) Goodwin, Z. A.; Feng, G.; Kornyshev, A. A. Mean-Field Theory of Electrical Double Layer In Ionic Liquids with Account of Short-Range Correlations. *Electrochim. Acta* **2017**, *225*, 190–197.

(12) Han, Y.; Huang, S.; Yan, T. A mean-field theory on the differential capacitance of asymmetric ionic liquid electrolytes. *J. Phys.: Condens. Matter* **2014**, *26*, 284103.

(13) Salanne, M.; Siqueira, L. J.; Seitsonen, A. P.; Madden, P. A.; Kirchner, B. From molten salts to room temperature ionic liquids: Simulation studies on chloroaluminate systems. *Faraday Discuss.* **2012**, *154*, 171–188.

(14) Feng, G.; Huang, J.; Sumpter, B. G.; Meunier, V.; Qiao, R. Structure and dynamics of electrical double layers in organic electrolytes. *Phys. Chem. Chem. Phys.* **2010**, *12*, 5468–5479.

(15) Shim, Y.; Jung, Y.; Kim, H. J. Graphene-based supercapacitors: A computer simulation study. *J. Phys. Chem. C* **2011**, *115*, 23574–23583.

(16) Jiang, D.-e.; Jin, Z.; Henderson, D.; Wu, J. Solvent effect on the pore-size dependence of an organic electrolyte supercapacitor. *J. Phys. Chem. Lett.* **2012**, *3*, 1727–1731.

(17) Merlet, C.; Salanne, M.; Rotenberg, B.; Madden, P. A. Influence of solvation on the structural and capacitive properties of electrical double layer capacitors. *Electrochim. Acta* **2013**, *101*, 262–271.

(18) Feng, G.; Jiang, X.; Qiao, R.; Kornyshev, A. A. Water in ionic liquids at electrified interfaces: The anatomy of electrosorption. *ACS Nano* **2014**, *8*, 11685–11694.

(19) Docampo-Álvarez, B.; Gómez-González, V.; Montes-Campos, H.; Otero-Mato, J. M.; Méndez-Morales, T.; Cabeza, O.; Gallego, L.; Lynden-Bell, R. M.; Ivaništšev, V. B.; Fedorov, M. V. Molecular dynamics simulation of the behaviour of water in nano-confined ionic liquid−water mixtures. *J. Phys.: Condens. Matter* **2016**, *28*, 464001.
(20) Cui, T.; Lahiri, A.; Carstens, T.; Borisenko, N.; Pulletikurthi, G.; Kuhl, C.; Endres, F. Influence of Water on the Electrified Ionic Liquid/Solid Interface: A Direct Observation of the Transition From a Multilayered Structure to a Double Layer Structure. *J. Phys. Chem. C* **2016**, *120*, 9341−9349.
(21) Wang, Y.; Chen, Y.; Gao, J.; Yoon, H. G.; Jin, L.; Forsyth, M.; Dingemans, T. J.; Madsen, L. A. Highly Conductive and Thermally Stable Ion Gels with Tunable Anisotropy and Modulus. *Adv. Mater.* **2016**, *28*, 2571−2578.
(22) Wang, Y.; Gao, J.; Dingemans, T. J.; Madsen, L. A. Molecular alignment and ion transport in rigid rod polyelectrolyte solutions. *Macromolecules* **2014**, *47*, 2984−2992.
(23) Yu, Z.; He, Y.; Wang, Y.; Madsen, L. A.; Qiao, R. Molecular Structure and Dynamics of Ionic Liquids in a Rigid-Rod Polyanion-Based Ion Gel. *Langmuir* **2017**, *33*, 322−331.
(24) Zhong, X.; Liu, Z.; Cao, D. Improved classical united-atom force field for imidazolium-based ionic liquids: tetrafluoroborate, hexafluorophosphate, methylsulfate, trifluoromethylsulfonate, acetate, trifluoroacetate, and bis (trifluoromethylsulfonyl) amide. *J. Phys. Chem. B* **2011**, *115*, 10027−10040.
(25) Jorgensen, W. L.; Maxwell, D. S.; Tirado-Rives, J. Development and testing of the OPLS all-atom force field on conformational energetics and properties of organic liquids. *J. Am. Chem. Soc.* **1996**, *118*, 11225−11236.
(26) Patra, M.; Karttunen, M. Systematic comparison of force fields for microscopic simulations of NaCl in aqueous solutions: diffusion, free energy of hydration, and structural properties. *J. Comput. Chem.* **2004**, *25*, 678−689.
(27) Hess, B.; Kutzner, C.; Van Der Spoel, D.; Lindahl, E. GROMACS 4: algorithms for highly efficient, load-balanced, and scalable molecular simulation. *J. Chem. Theory Comput.* **2008**, *4*, 435−447.
(28) Bussi, G.; Donadio, D.; Parrinello, M. Canonical sampling through velocity rescaling. *J. Chem. Phys.* **2007**, *126*, 014101.
(29) Hess, B.; Bekker, H.; Berendsen, H. J.; Fraaije, J. G. LINCS: a linear constraint solver for molecular simulations. *J. Comput. Chem.* **1997**, *18*, 1463−1472.
(30) Torrie, G. M.; Valleau, J. P. Monte Carlo free energy estimates using non-Boltzmann sampling: application to the sub-critical Lennard-Jones fluid. *Chem. Phys. Lett.* **1974**, *28*, 578−581.
(31) Kumar, S.; Rosenberg, J. M.; Bouzida, D.; Swendsen, R. H.; Kollman, P. A. The weighted histogram analysis method for free-energy calculations on biomolecules. I. The method. *J. Comput. Chem.* **1992**, *13*, 1011−1021.
(32) Hub, J. S.; De Groot, B. L.; Van Der Spoel, D. g_wham A Free Weighted Histogram Analysis Implementation Including Robust Error and Autocorrelation Estimates. *J. Chem. Theory Comput.* **2010**, *6*, 3713−3720.
(33) Feng, G.; Zhang, J.; Qiao, R. Microstructure and capacitance of the electrical double layers at the interface of ionic liquids and planar electrodes. *J. Phys. Chem. C* **2009**, *113*, 4549−4559.
(34) Grosberg, A. Y.; Nguyen, T.; Shklovskii, B. Colloquium: the physics of charge inversion in chemical and biological systems. *Rev. Mod. Phys.* **2002**, *74*, 329.

DOI: 10.1021/acs.jpcc.7b02466
J. Phys. Chem. C 2017, 121, 9454−9461